Methodology and computational implementation of a New Zealand Velocity Model (NZVM2.0) for broadband ground motion simulation

Ethan M. Thomson, Brendon A. Bradley & Robin L. Lee

Taylor & Francis
Taylor & Francis Group

RESEARCH ARTICLE

Check for updates

Methodology and computational implementation of a New Zealand Velocity Model (NZVM2.0) for broadband ground motion simulation

Ethan M. Thomson, Brendon A. Bradley and Robin L. Lee

Department of Civil and Natural Resources Engineering, University of Canterbury, Canterbury, New Zealand

ABSTRACT

This paper presents a generalised velocity model construction methodology, its computational implementation, and application in the construction of a New Zealand Velocity Model (NZVM2.0) for use in physics-based broadband ground motion simulation. The methodology utilises multiple datasets spanning different length scales, which is enabled via the use of modular subregions, geologic surfaces, and parametric representations of crustal velocity. A number of efficiency-related workflows to decrease the overall computational construction time are employed, while maintaining the flexibility and extensibility to incorporate additional datasets and refined velocity parameterisations as they become available. The methodology and computational implementation processes are then applied for development of a New Zealand Velocity Model (NZVM2.0) for use in broadband ground motion simulation. The model comprises explicit representations of the Canterbury, Wellington, Nelson-Tasman, Kaikōura, Marlborough, Waiau, Hanmer and Cheviot sedimentary basins embedded within an existing regional travel-time tomography-based velocity model for the shallow crust.

Introduction

In recent years, physics-based methods have been increasingly used for earthquake-induced ground motion simulations following rapid advancements in high performance computing, and subsequently seismic source and crustal modelling. Three dimensional crustal models are an integral part of earthquake-induced ground motion simulation methods, in which the crustal model defines the computational domain over which the wave equation is solved to determine strong ground motion shaking. Such models are often also referred to colloquially as 'velocity models' because viscoelastic simulations require only P- and S-wave velocities, along with density, and anelastic attenuation, and the latter two parameters are often inferred from correlations with velocity (Süss and Shaw 2003; Taborda 2014). These parameters collectively enable the three-dimensional viscoelastic wave equation to be solved at frequencies of engineering interest.

Velocity models have been constructed for numerous regions globally, with varying complexity, and have employed a number of different methodologies in their development. For physics-based ground motion simulation, representation of impedance contrasts is paramount in order to adequately capture wave and amplitude reverberations. Therefore, explicitly modelling these contrasts, which typically occur in sedimentary basins, is of high importance. Travel-time-derived velocity models (e.g. Eberhart-Phillips et al. (2010); used principally in earthquake location studies) fail to adequately capture these impedance contrasts and therefore by themselves are insufficient for use in such ground motion simulations. In order to explicitly capture impedance contrasts, a core component in velocity model construction is often the use of geologic surfaces to delineate between differing geologic materials such as the interfaces between sedimentary deposits and underlying basement rock, or the boundary between differing lithological units. Between these surfaces velocities are prescribed according to a predefined set of rules.

The geologic surface-based approach has been used in the construction of velocity models for a number of regions, including the Osaka basin in Japan (Kagawa et al. 2004), the Rhone Valley in Southern France (Roten et al. 2008) and the Mygdonian Basin in Greece (Maufroy et al. 2015), each of which utilise a geologic surface to define the sediment-basement interface. Above this basement-sediment surface a 1D velocity structure is defined, with the basement characterised as a homogeneous material. However, basement models are not restricted to homogeneous characterisation, for example, the velocity models for the Grenoble Valley in France (Chaljub et al. 2015) and the Adaoazari Basin in Turkey (Goto et al. 2005) utilise a 1D velocity structure (i.e. laterally homogeneous at constant depths) to prescribe basement velocities.

Numerous velocity models embed 3D basin models within regional crustal models that prescribe velocities within the geologic basement. This approach is utilised for: the Po Plain Sedimentary Basin in Italy (Molinari et al. 2015), which embeds a 3D basin model within a crustal model of the European Plate (Molinari and Morelli 2011); a velocity model of the Puget Sound in Washington State USA (Frankel and Stephenson 2000; Pitarka et al. 2004) embeds a basin model within the hybrid tomography and gravity model of Parsons et al. (2001); and two Southern California Community Velocity Models (CVM), CVM-H (Süss and Shaw 2003; Shaw et al. 2015), and CVM-S (Magistrale et al. 2000, 1996; Kohler et al. 2003; Lee et al. 2014), which embed 3D sedimentary basin models within the 3D crustal model of Hauksson and Haase (1997).

Beyond geologic surfaces for basement definition alone, velocity models can utilise multiple geologic surfaces and multiple basins in their construction; a velocity model of the Central United States (CUSVM) (Ramírez-Guzmán et al. 2012) prescribes multiple geologic surfaces over the entire model domain, between which depth-dependent functions are used to characterise velocities. Velocity models of the Adaoazari Basin in Turkey (Goto et al. 2005), and Puget Sound USA (Frankel and Stephenson 2000; Pitarka et al. 2004), utilise numerous surfaces to delineate between geologic formations within the modelled sedimentary basins. Southern California CVMs characterise multiple sedimentary basins, the primary difference between CVM-S (Magistrale et al. 2000, 1996; Kohler et al. 2003; Lee et al. 2014) and CVM-H (Süss and Shaw 2003; Shaw et al. 2015), is that the former utilises parametric functions to prescribe basin velocities, while the latter utilises a 3D velocity field developed by geospatial kriging of sonic logs and seismic reflection data to characterise basin velocities.

An alternative approach to the aforementioned velocity model construction methodologies has been implemented within a model of the San Francisco Bay Area in Northern California (Rodgers et al. 2008). This model defines a number of discrete 3D geologic blocks (i.e. volumes) and prescribes velocities within each block using geology-specific velocity parameterisations, as opposed to continuous full-domain geologic surfaces previously noted. While full domain surfaces allow only one continuous basin to be defined, modelling discrete 3D volumes allows for multiple basins or subregions to be defined and inserted within geologic basement models.

The need for multi-scale resolution of velocity models arises from the requirements to numerically model (relatively) high frequency wave propagation, yet consider large geographical regions. As a result, multiple datasets, often obtained from various acquisition and analysis methods, are used to obtain the best available representation of crustal properties over the region of interest. The utilisation of such models in numerical simulations also requires different input and output formats associated with the use of different numerical algorithms for solution. Hence, the methodology and computational implementation by which crustal velocity models are constructed is important to ensure they are fit for present purpose, but also easily extensible to handle additional datasets and numerical methods. Existing literature on developed velocity models have arguably not extensively detailed their computational implementations, and this paper therefore seeks to present the details of computational implementation and velocity model methodology, which integrates the approaches considered in the previous literature review with the flexibility to incorporate new datasets in the future. Specific attention is given to discussion of this method and its computational implementation in order to assist in its application by others.

In the following sections we present the details of a velocity model methodology, its computational implementation, and subsequent application to construct a model for New Zealand for use in broadband ground motion simulation. Multiple datasets amassed from numerous geophysical and geological studies are employed in the construction of several subregions, and these discrete regional models are then embedded within a (relatively) lower resolution New Zealand-wide travel-time-derived tomography model (Eberhart-Phillips et al. 2010). The resulting velocity model incorporates data across multiple length scales and resolutions to give a unified representation of the velocity structure for use in broadband physics-based ground motion simulations and additional engineering applications.

Velocity model methodology

Seismic velocity information can be obtained via geotechnical, geological and geophysical approaches and techniques, and span a range of geographic regions, length scales, spatial density, and quality. To appropriately represent areas of variable data resolution, a 'subregion' approach is useful, where specific datasets and subsequent modelling assumptions are applied within fully enclosed volumes. This approach combines the geologic surface methods (e.g. Magistrale et al. 1996; Ramírez-Guzmán et al. 2012) with technique of discrete geologic volumes (e.g. Süss and Shaw 2003; Rodgers et al. 2008). In addition, where appropriate, a surface-based method is also instructive, in which 3D geologic surfaces enable the 3D continuum to be separated into distinct lithological units for subsequent velocity parametrisation. The concepts of subregions and surface-based modelling are the foundation of the

flexible and extensible velocity model construction presented here.

Figure 1 illustrates the three steps required to prescribe velocities at a specific point defined by latitude, longitude and depth. In summary, firstly, the latitude-longitude coordinates are utilised to determine whether the point lies within a specific subregion. Secondly, surface-based modelling is employed to determine the geologic surfaces that bound the point in the vertical coordinate, and hence the lithological unit that the point resides in. Finally, the velocity parametrisation within the identified lithological unit is used to compute the resulting velocities. The following three subsections discuss the methodological specifics for each of these primary steps, with the computational implementation discussed separately in Section 3.

Subregions

Subregions are 3D volumes within the velocity model that have region-specific parameterisations for the computation of velocities. Data quality and quantity can vary by region, thus by constructing subregions it is possible to utilise region-specific datasets when constructing a velocity model. Examples include sedimentary basins, which have large variations in velocity properties over short spatial scales that are not captured explicitly in coarse regional-scale 3D velocity models used for earthquake location. It would also be expected that there is a greater need for high-spatial resolution modelling in areas of higher population density, where seismic risk exposure is high.

A two-step process can be implemented for determining if a point lies within a specific subregion, in which first the location is checked in the latitude-longitude plane to determine if it lies within the subregion boundary, and if so, then secondly examining the depth of the point with respect to the top and bottom subregion surfaces for the corresponding latitude-longitude. Figure 2 provides a schematic illustration of the three possible scenarios when determining if a gridpoint lies within a sub-region: (i) outside the subregion boundary; (ii) inside the surface projection of

the subregion but outside the depth range; and (iii) inside the sub-region. The computational distinction between these three cases is discussed in Section 3.2.

Bounding surfaces

The bounding surfaces concept, with top and bottom surfaces to characterise the vertical extent of a lithological unit, enables each geologic layer to be modelled discretely and distinct velocity parameterisations to be applied to each layer. Figure 3 illustrates the process for determining which unit a point lies within. First the appropriate geologic surfaces are interpolated at the latitude-longitude of the point, then the two surfaces that bound the gridpoint in the vertical direction are determined.

The concept of bounding surfaces can be applied at both the subregion and 'global' (i.e. regional) scale when constructing a velocity model. At the subregion scale, surfaces can be used to define the top, intermediary and bottom surfaces of a subregion, while at the global level it can it can be utilised in prescribing full domain surfaces, such as the ground surface elevation and the Moho discontinuity (e.g. Kohler et al. 2003), among others. The computational implementation of bounding surface determination is presented in Section 3.2.2.

Calculation of velocities within a unit

A velocity parametrisation, specific to an individual geologic unit, is used to prescribe the required crustal characteristics to a point. Figure 4 illustrates various velocity parametrisations, ranging from simple prescription of constant velocities to interpolation of three-dimensional fields. For example, the CVM-H model of Los Angeles (Süss and Shaw 2003; Shaw et al. 2015) uses geospatial kriging of multiple seismic reflections lines to construct a 3D velocity field. Whereas other velocity models, CVM-S (Magistrale et al. 2000, 1996; Kohler et al. 2003; Lee et al. 2014), USGS Bay Area (Rodgers et al. 2008), and CUSVM
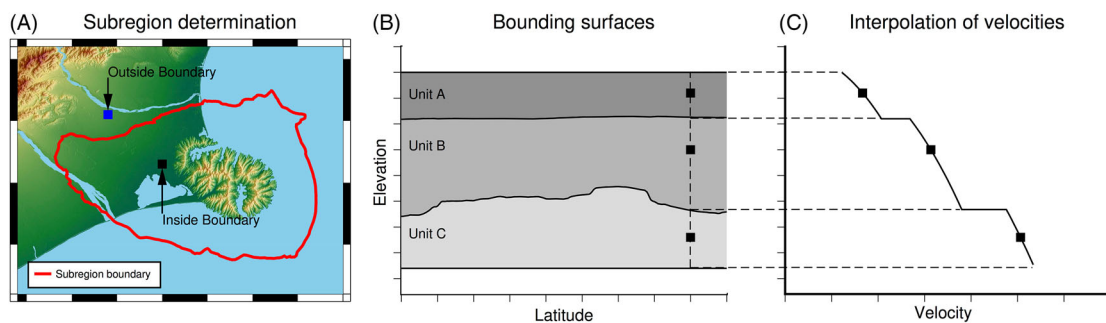

Figure 1. Conceptual overview of the steps to prescribe velocities at a point: **A**, determining which subregion (if any) the point resides in; **B**, interpolation of applicable geologic surfaces to identify those that vertically 'bound' the point, and hence determine the lithological unit; and **C**, prescription of velocities using velocity parameterisation specific to the lithological unit.
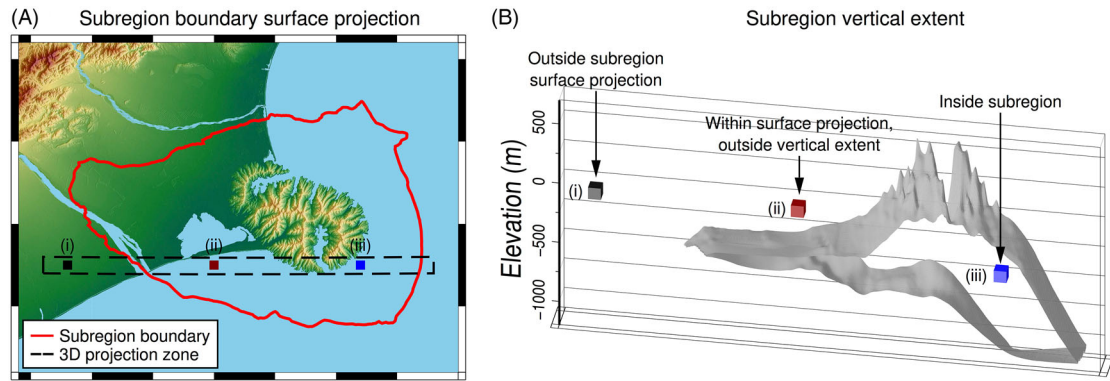
Figure 2. Schematic illustration of the two-step process used to determine if a point lies within a subregion. Gridpoint location is compared with **A**, the surface projection of the subregion boundary and **B**, The top and bottom subregion surfaces. Example points. (i) (ii) and (iii) illustrate the possible outcomes for the example of the Banks Peninsula volcanics subregion within the NZVM discussed in Section 4.2.2.
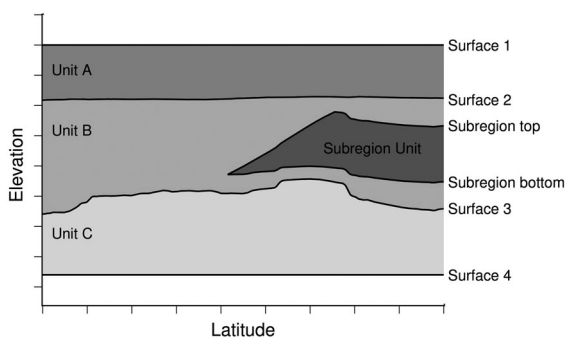

Figure 3. Schematic illustration of how bounding surfaces are used to delineate the boundaries between differing geologic units, allowing for different velocity parameterisations to be applied to geologically distinct units. E.g. a gridpoint bounded by Surface 1 and Surface 2 lies within geologic Unit A, while a gridpoint bounded by the Subregion top and Subregion Bottom surfaces lies within the Subregion geologic unit.

(Ramírez-Guzmán et al. 2012) utilise parametric functions calibrated based on available data.

Velocity parametrisations can take on any functional form and can utilise any number of inputs depending on the quality and quantity of data available in their construction – the data availability will naturally influence which velocity parameterisation is optimal. This allows for the effect of: age, composition,

weathering, overburden stress and a multitude of other factors to be explicitly considered when prescribing velocities.

The determination of an appropriate velocity parametrisation is not always selfevident and ground motion simulation validation using observed recordings from historical earthquakes is the most robust manner to understand resulting model validity. For example, ground motion simulations conducted using both CVM models for the 2008 Chino Hills earthquake (Taborda and Bielak 2014) have illustrated that simulated waveforms from the parametric CVM-S model are significantly closer to observed motions than those obtained from the 3D interpolated CVM-H model. Such findings highlight the potential problems that may occur when using a data-driven model without explicit validation of the resulting predicted waveforms.

Frequently only the P-wave velocity, V_p is specified. With S-wave velocity, V_s; and density, ρ being derived from empirical correlations (e.g. Brocher 2005). Quality factors for viscoelastic wave propagation can similarly be obtained from correlations (e.g. Süss and Shaw 2003; Taborda 2014); although nonlinear wave propagation simulations have been undertaken (Roten et al. 2014), these are currently in their infancy,
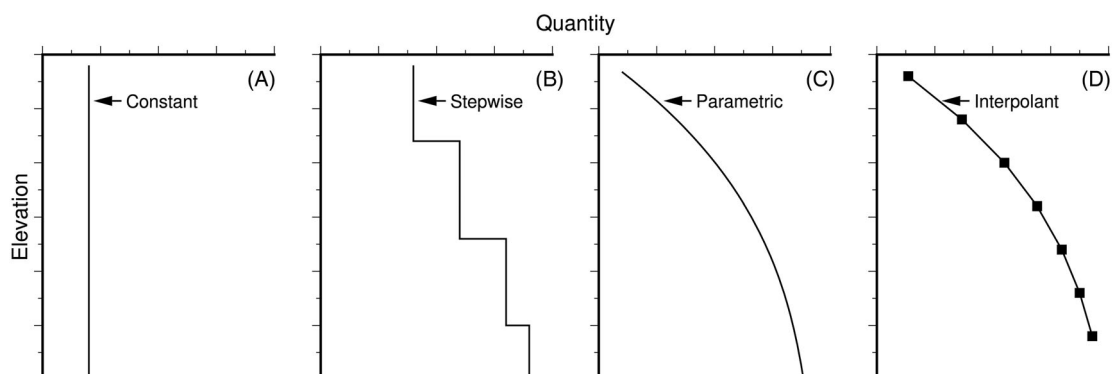

Figure 4. Examples of typical velocity parametrisations used to prescribe quantities (V_p, V_s and ρ) within a geologic unit. While these illustrations are shown in 2D for conceptual simplicity, they are all applicable in 3D.

so explicit discussion of nonlinear parameters such as cohesion and friction angle is omitted here.

Representation of surface topography

Several implemented numerical solution schemes for ground motion simulation are able to explicitly model ground surface topography (e.g. Komatitsch and Tromp 1999; Aagaard et al. 2001; Olsen et al. 2006; Tu et al. 2006) while others utilise a flat free surface (e.g. Graves 1996; Cui et al. 2010). Figure 5 illustrates four general types of topographic representation, which we refer to as: (i) True; (ii) Bulldozed; (iii) Squashed; and (iv) Squashed-Tapered. As the name suggests, (i) represents the actual surface topography (Figure 5A). When a flat free-surface is required, the Bulldozed approach (Figure 5B) simply ignores surface topography and obtains the free-surface values corresponding to a constant reference elevation. In regions where the surface elevation varies appreciably, the use of a Bulldozed approach can be problematic because it will result in significant near surface crustal properties being neglected, which is problematic in locations where elevations are substantially different than the reference elevation used. An alternative is to enforce a flat free-surface by squashing the surface topography (Figure 5C). Computationally, this simply requires extracting velocities based on the depth of the point below the surface elevation, as opposed to the Bulldozed representation where depths are relative to a constant reference elevation. Aagaard et al. (2008) performed ground motion simulations of the 1989 Loma Prieta Earthquake using a variety of

different topographic representations, and found the Bulldozed representation performed relatively poorly compared with Squashed and Squashed-Tapered representations at matching observed ground motions, potentially due to near surface low velocity material being omitted from the velocity model.

As shown in Figure 5, the downside of the squashed representation is the distortion of the subsurface in order to achieve a flat-layered free surface. The squashed-tapered representation (Figure 5D) aims to achieve the benefits of the squashed representation at accounting for the near-surface, without significant subsurface distortions. This is achieved by tapering the effect of the 'squashing' as the depth increases. An example where the squashed-tapered approach has been adopted can be seen in Harmsen et al. (2008).

The mathematical representation for the effective elevation ($z_{effective}$) of a point for squashed and squashed-tapered representations is:

$$z_{effective} = z_{actual} - \alpha \times z_{DEM} \quad (1)$$

where z_{actual} is the original elevation of the point relative to a reference datum, z_{DEM} is the depth of the DEM (digital elevation model, i.e. the ground surface) and α is the shift multiplier. For the squashed representation, $\alpha = 1$. For the squashed-tapered representation we define the multiplier by the following equation:

$$\alpha = \max\left\{ 1 - \frac{z_{reference} - z_{actual}}{\beta \times z_{DEM}}, 0 \right\} \quad (2)$$

where $\beta\, z_{DEM}$ is the distance over which a linear taper is applied (alternative tapering functions could also be
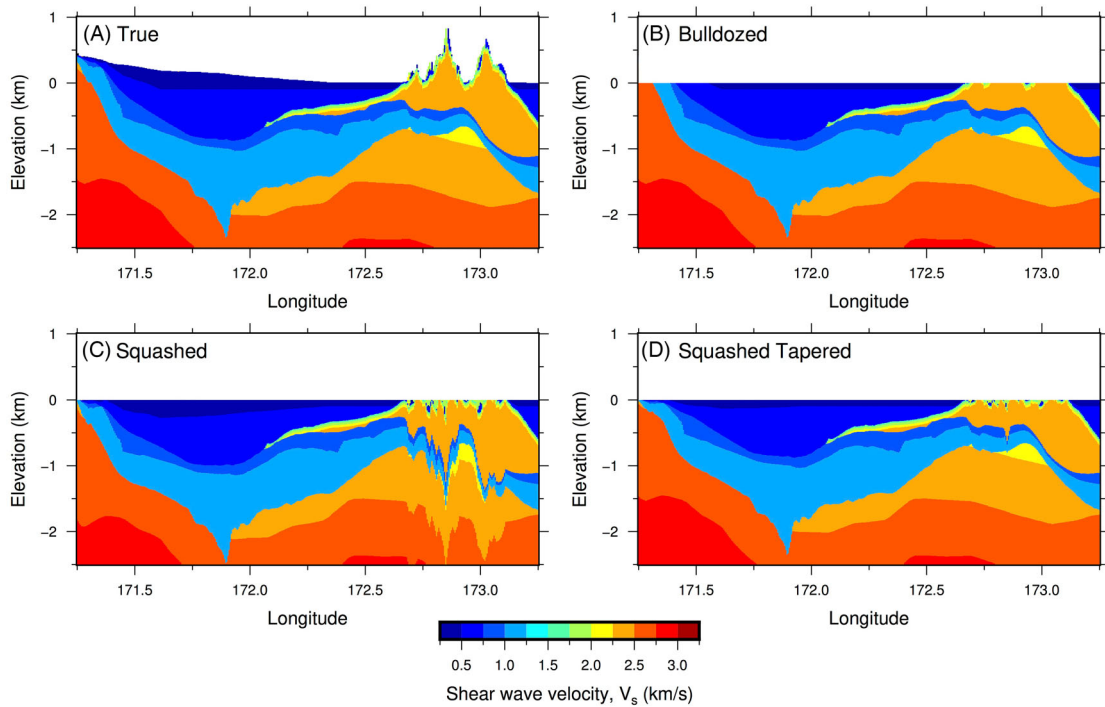

Figure 5. Illustration of four types of topography representation: **A,** true, **B,** bulldozed, **C,** squashed and **D,** squashed-tapered (for $\beta = 1$), for an east-west transect through Banks Peninsula, as shown in Figure 2.

adopted) and $z_{reference}$ is the constant reference depth for which the shifted points are relative to. From the functional form in Equation (2) it can be seen that the tapering ceases when $\frac{z_{reference} - z_{actual}}{\beta \times z_{DEM}} = 1$. Typical values of β are 1–3.

Computational implementation

Ground motion simulation utilising crustal velocity models often requires significant high performance computing (HPC) resources (e.g. velocity models typically cover large regions and contain 10^6 10^{12} spatial gridpoints, Cui et al. 2010). As a result, the consideration of computational efficiency and parallelisation during implementation and execution of velocity models is important to ensure that they are able to handle the computational and data demands of HPC. The computational implementations of previous velocity models: CVM-S (Magistrale et al. 2000, 1996; Kohler et al. 2003; Lee et al. 2014), CVM-H (Süss and Shaw 2003; Shaw et al. 2015), USGS Bay Area (Rodgers et al. 2008) and CUSVM (Ramírez-Guzmán et al. 2012) are not documented. This section presents the overall computational workflow for velocity model construction, enabling researchers to utilise this methodology to construct velocity models of new regions globally (see Data and resources for source code).

Figure 6 illustrates the high-level processes for constructing a velocity model for use in ground-motion simulation on a computational domain. Herein focus is given to structured meshes, although separate meshing software can be integrated into this workflow to generate velocity models on unstructured meshes. Pseudo-code is used in the following paragraphs to convey the names and intentions of files and processes for the purpose of conveying the computational workflow.

Input data preparation

Figure 6 illustrates the three primary steps required to generate velocity model input data. First, the structured mesh is generated within a function *generateModelGrid* which builds a mesh in the Cartesian domain using the length of the model in three orthogonal directions and the spacing between gridpoints. This Cartesian grid is then mapped to the latitude-longitude domain using a coordinate transformation. This allows the user to specify the coverage region of the velocity model and to set the grid spacing to the desired resolution. Second, via a version number, the names of the specific resources (subregions, surfaces and velocity parameterisations to be used in velocity model construction) are obtained using a *getGlobalModelParameters* function. The use of version numbering allows for multiple variants of velocity models to be generated using the same body of code to be compared and contrasted. Finally,

using the version-specific resources obtained in the previous step, all required data is loaded into memory by a *loadAllData* function. This function first loads all applicable global data, surfaces and velocity parameterisations that apply over the entire domain. This is followed by subregion-specific resources; surfaces, boundaries and velocity parameterisations. After these preliminary steps are complete, the grid points at which crustal properties are desired can then be looped over and have their velocities prescribed using the three primary steps presented in Section 2.

Implementation

This section details the computational workflow for velocity model construction using the three primary steps as outlined in Sections 2.1–2.3. The implementation is presented with application to prescribing the velocities to a vector of points representing grid points at different depths for a single latitude-longitude coordinate.

Subregion determination

As detailed in Section 2.1, it is necessary to determine if a gridpoint is within any subregion in order to apply the appropriate velocity parameterisation. Figure 7A presents the computational workflow and functions required to determine if a gridpoint lies within a given subregion. As multiple subregions can be implemented within a single velocity model, this process is repeated for each and every subregion.

From a subregion boundary and bounding surfaces, a two-step process can be implemented to resolve the gridpoint's location with respect to the 3D subregion. A function *determineSubregionSurfaceDepths* first checks the latitude and longitude location of the gridpoint against the surface projection of the subregion. If the gridpoint is within this projection, the subregion surface depths are interpolated within *determineSubregionSurfaceDepths* and compared against the depths within the vector of gridpoints. To minimise computation, subregion surface depths are interpolated only once and can then be stored in memory for use is subsequent computations for all gridpoints at a given latitude-longitude.

Bounding surfaces

Figure 7B presents the computational workflow for determining which surfaces, either subregion or full domain, bound a gridpoint. The concept of bounding surfaces is discussed in Section 2.2. After determining whether the gridpoint is located within an implemented subregion or not, the appropriate geologic surfaces, full domain and/or subregion, are identified. Each of these surfaces are then interpolated and compared with the depths of each gridpoint to determine the bounding surfaces (the surfaces immediately above and below the gridpoint). If the gridpoint lies
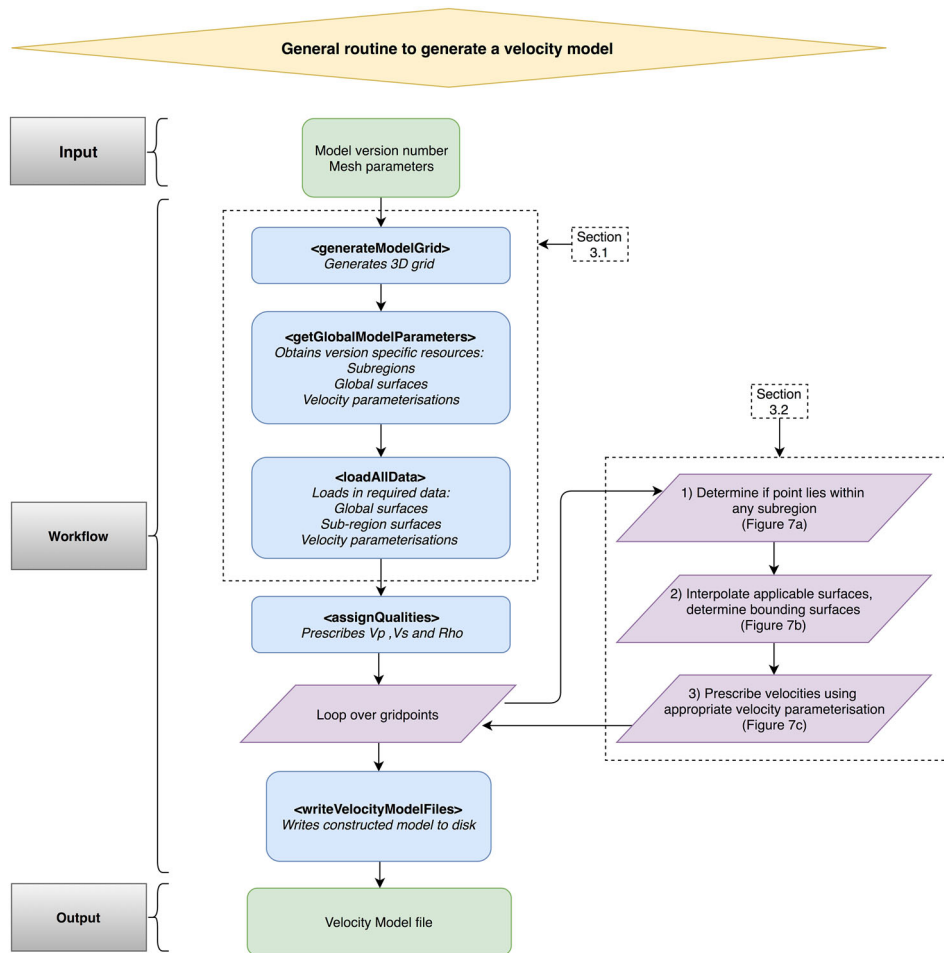
Figure 6. High-level computational process for constructing a velocity model for use in physics based ground motion simulation.

outside of all subregions, then the geologic surface depths are calculated within *interpolateGlobalSurface-Depths*, however if the gridpoint is within a subregion then the surface depths have previously been interpolated and can be loaded from memory.

To ensure the interpolated surface depths are consistent with current understanding of regional stratigraphy it necessary to check the interpolated surfaced depths. This is due to the geospatial interpolation methods used to develop the geologic surfaces which
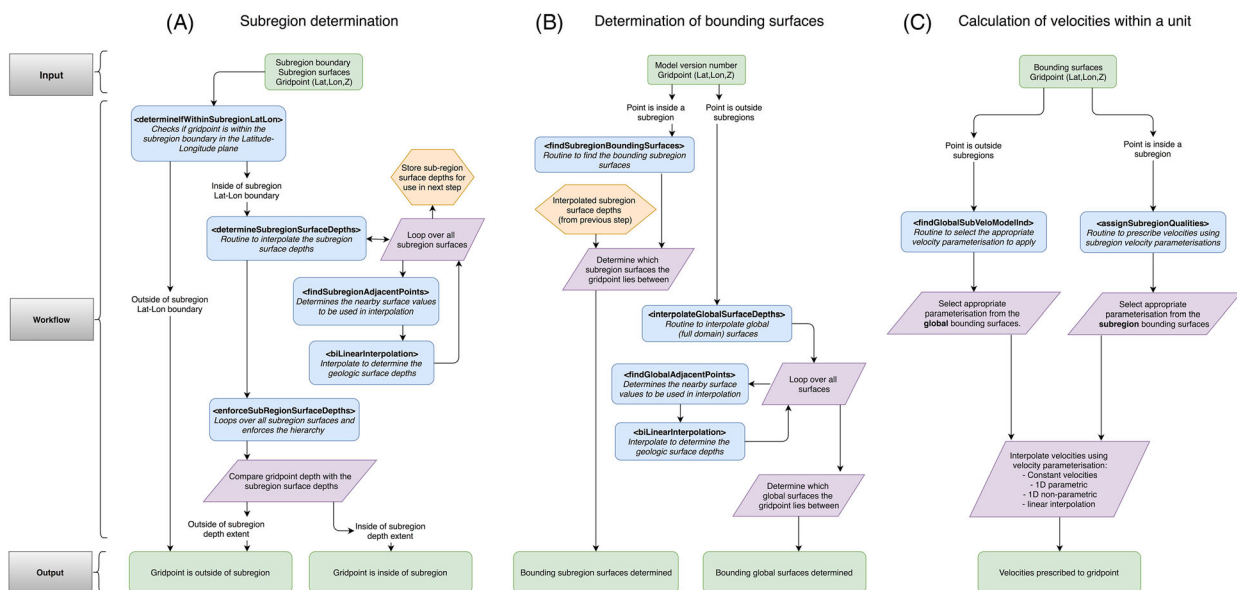

Figure 7. Computational processes used to prescribe velocities to a gridpoint: **A,** determine if a point lies within a specific subregion, **B,** interpolation of applicable surfaces at a gridpoint and **C,** prescription of velocities using a velocity parameterisation.

can result in surfaces, which delineate geologic unit boundaries, crossing over one another. This is remedied by enforcing the surfaces to ensure their interpolated values are consistent with apriori knowledge of stratigraphy.

Calculating velocities within a unit

From the bounding surfaces for a gridpoint the appropriate velocity parameterisation can be selected and used to prescribe velocities. As discussed conceptually in Section 2.3, velocity parameterisations can take on several different functional forms ranging from the prescription of constant velocities to interpolants of 3D velocity fields, such as regional crustal models developed by tomographic inversion. The computational workflow for prescribing velocities to a gridpoint is presented in Figure 7C.

Representation of surface topography

The four topographic representations discussed in Section 2.4 have been implemented within the NZVM source code. Prescription of velocities for the True and Bulldozed representations (see Figure 5) involves prescribing velocities at the exact latitude, longitude and depth of the gridpoint. The difference between True and Bulldozed is that the former prescribes velocities to gridpoints below the DEM whereas the latter prescribes velocities relative to a constant reference depth resulting in a flat free-surface. This is achieved through simple *if* statements which prescribe the velocities as not-a-number (*NaNs*) if a gridpoint lies above the DEM for the True representation, or above the reference depth for the Bulldozed representation. For the Squashed and Squashed-Tapered representations the depth of a given gridpoint is shifted vertically, this is achieved by reassigning the depth according to Equation (1). Velocities are then prescribed to the vector of depth-reassigned gridpoints which are then mapped back to the vector of original depths.

Efficiency processes and algorithms

Due to limitations on computational processing power, a number of efficiency-related algorithms and processes have been implemented to reduce the computational effort and the wall clock duration required to generate a velocity model by orders of magnitude. Three areas targeted for efficiency gains were parallelisation, data storage and efficient algorithms. Using pre-existing libraries (e.g. Message Passing Interface, MPI) and tools, repetitive computational processes can be performed in parallel.

Geologic surfaces are stored in raster format with their coordinates defined by vectors of latitudes and longitudes. Using vectors to characterise surfaces enables computationally efficient determination of the quadrant within the surface which the gridpoint lies, which can be subsequently used in a bilinear interpolation process to obtain the surface depths at the queried gridpoint in question. A similar approach is utilised to prescribe the regional tomographic model, velocities are stored at multiple planes at constant depths, enabling which depth planes and quadrants a gridpoint lies within to be easily identified, and a tri-linear interpolation process to determine the velocity at the gridpoint. Ray casting is an efficient algorithm that can be applied to determine if a gridpoint lies within a polygon, this is algorithm is utilised to determine if a gridpoint lies within a subregion boundary.

Visual verification techniques

Good programming practice dictates that functions are verified using numerous test cases as they are written. In addition to low-level verification of velocity model functions, it is possible to verify the procedures used in velocity model construction. By constructing the velocity model in steps starting with an individual gridpoint, progressing to a one-dimensional profile, then two-dimensional slice and finally a three-dimensional mesh, we are able to verify the full velocity model source code functions. A final step in verifying the velocity model implementation is to interpolate velocity transects through a saved model. Figure 8 illustrates a velocity slice interpolated through a saved velocity model, generated for use in ground motion simulation. Interpolating multiple velocity transects through a saved velocity model enables the geologic structure, to be investigated visually. Because velocity models are infinitely complex this step cannot be automated and therefore human intervention can always be useful to confirm the velocity models files are satisfactory for use in ground motion simulation.

Development of a New Zealand velocity model

Using the methodology and computational implementation presented in previous sections, a velocity model for New Zealand (NZVM) was constructed for use in physics-based ground motion simulation as presented herein. The model utilises a travel-time-derived tomographic model of New Zealand (Eberhart-Phillips et al. 2010) embedded with numerous sub-region models. The NZVM is modular, allowing for sub-regions within New Zealand to be added in future updates.

Intermediate versions of the model presented here included basin characterisation for only the Canterbury region (Lee, Bradley, et al. 2017) and were utilised in numerous ground motion simulations of historic earthquakes: 14 November 2016 Kaikōura (Bradley, Razafindrakoto, et al. 2017); 22 Feburary 2011
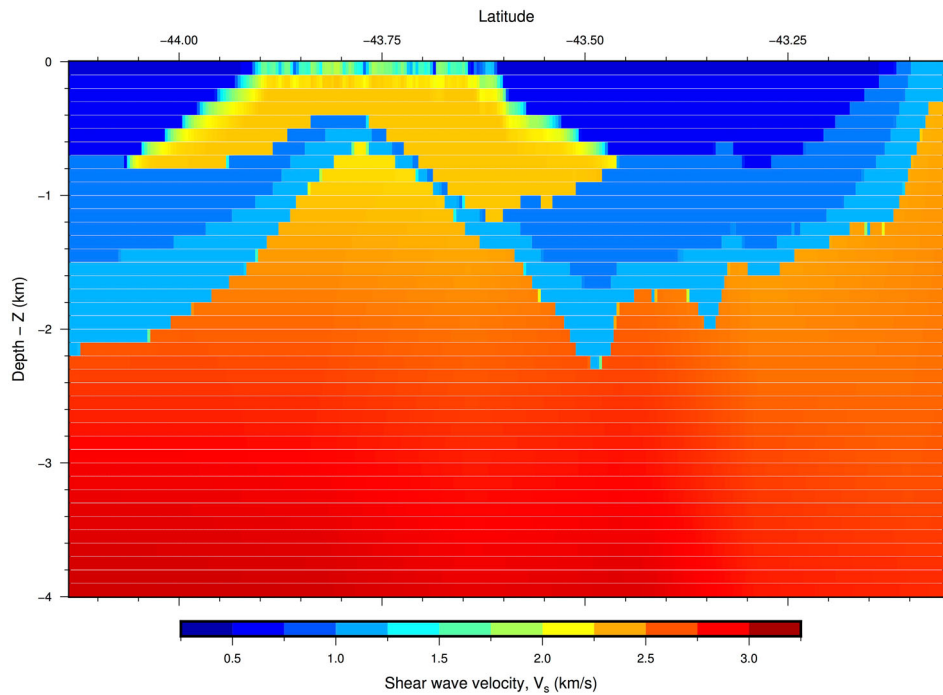
Figure 8. Velocity transect through a velocity model for the Canterbury region generated for use in ground motion simulation illustrating the as-saved velocity structure for visual verification. This model utilises a 100 m finite-difference grid which is apparent in both the horizontal and vertical directions.

Christchurch (Razafindrakoto et al. 2018); and small to moderate magnitude historic earthquakes for validation purposes (Lee et al. 2018); and potential future future earthquakes (Bradley, Bae, et al. 2017). We refer to those intermediate versions as NZVM1.0.

NZVM version 2.0 (NZVM2.0), presented here, builds on NZVM1.0 by incorporating seven new modular sedimentary basin models with varying degrees of characterisation. Figure 9 presents the domain of the NZVM2.0, including the subregions explicitly incorporated, and the locations of the planned additions given the modularity of the framework. The following subsections detail the datasets used in the construction of the NZVM2.0, and the available output formats (see Data and resources for the NZVM source code).

Regional crustal model

The Eberhart-Phillips et al. (2010) regional seismic velocity model was assembled using results from previous 3D travel-time inversion studies throughout New Zealand. In regions of low seismicity, where little or no ground motion recordings were available, alternative data sources were used (Wood and Woodward 2002; Horspool et al. 2006; Davy et al. 2008; Barker et al. 2009) in splicing together a New Zealand wide model. The model was then updated using travel-time data spanning across different spliced regions to ensure consistency throughout the modelled region.

Figure 10 illustrates the shear wave velocity structure at depths of three and eight kilometres derived

from the Eberhart-Phillips et al. (2010) seismic velocity model. The lateral resolution of the model is spatially coarse, ranging from 10 to 50 km by region, and the general trend of increasing shear wave velocity with depth is apparent. The model prescribes V_p, V_s and ρ at 22 depth planes ranging from 15 km above mean sea level (for interpolation purposes) to a depth of 750 km. Of particular interest for ground motion
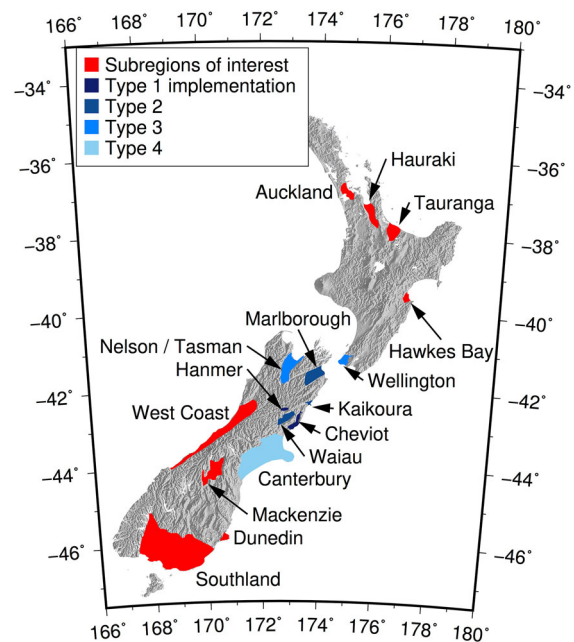

Figure 9. Subregions characterised in NZVM2.0 with varying degrees of complexity (Type 1–4) and other subregions of interest to be added in a future version.
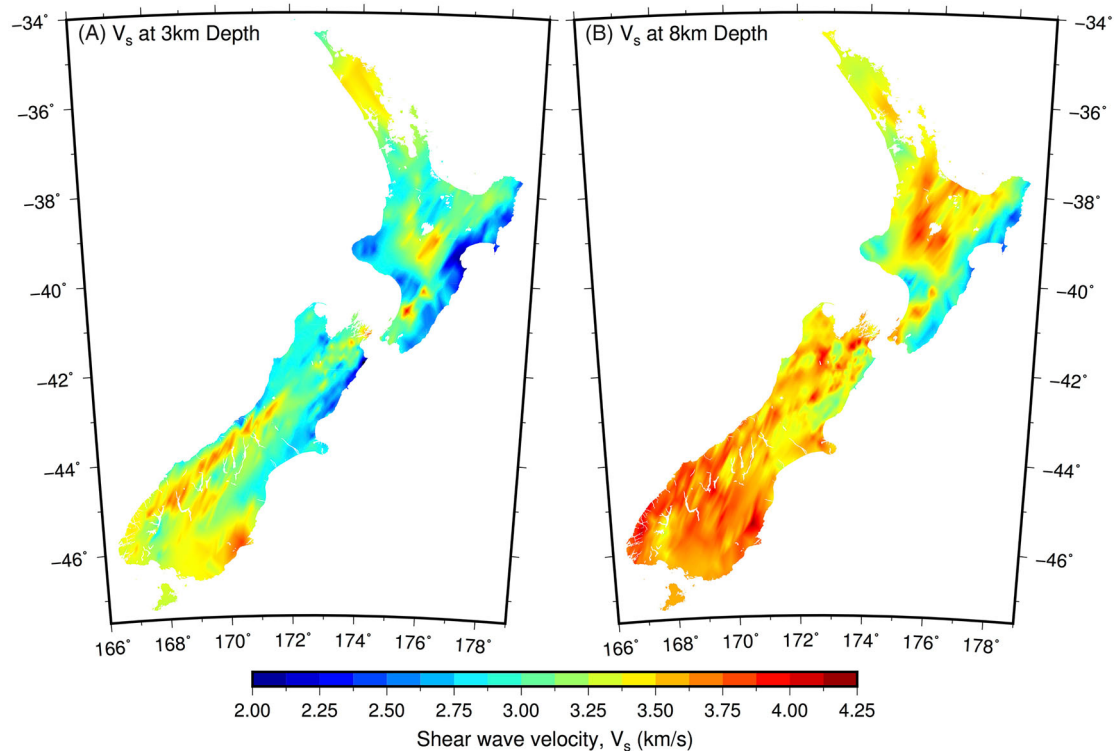
Figure 10. Shear wave velocities extracted at depths of: **A,** three and, **B,** eight kilometres from the regional crustal model of Eberhart-Phillips et al. (2010).

simulation is the characterisation of the shallow crust, and the depth planes above 30 km are 3, 8, 15, 23 and 30 km. For implementation within the NZVM each depth plane was interpolated onto a grid defined by latitude and longitude vectors.

Figure 11 presents a velocity fence diagram with multiple velocity transects through the Eberhart-Phillips et al. (2010) regional crustal model. The smooth variation of velocities with depth is highly apparent, additionally the minimum shear wave velocity prescribed by the model is relatively high ($V_s = 2.0$ km/s). This highlights the importance of characterising near-surface velocities and sedimentary deposits, which have significantly lower velocities than those present within the Eberhart-Phillips et al. (2010) model.

Subregion models

Eight subregion models classified into four characterisation types are implemented in NZVM2.0, Table 1 presents the features of each subregion type. Section 4.2.1 details the Type 1–3 subregion models while Section 4.2.2 presents the implementation of the Type 4 Canterbury subregion.

Type 1–3 subregion implementations

Type 1–3 subregion models, developed specifically for NZVM2.0, are implemented as volumes constrained by two surface models and a two-dimensional boundary. The bottom surface (i.e. the geologic basement) for these subregions was developed through geospatial Kriging, while the top surface is derived from a digital elevation model. Region specific geologic information were utilised in the construction of NZVM2.0 subregions: the Hanmer, Cheviot, Waiau and Kaikōura subregions utilised the Rattenbury et al. (2006) model; the Marlborough and Nelson-Tasman utilised the Rattenbury et al. (1998) model; and the Wellington region utilised the Begg and Johnston (2000) model. Additionally a Wellington model (Semmens et al. 2010) and Nelson-Tasman site characterisation study (McMahon and Wotherspoon 2017) were utilised as constraints in developing these subregions. Figure 12 presents a transect through the Waiau subregion, a Type 2 characterisation with a one-dimensional velocity parametrisation.

Velocity model for the Canterbury region, a Type 4 subregion

The 2010–2011 Canterbury earthquake sequence prompted a large body of work to detail the geologic structure of the Canterbury region. Therefore, detailed geologic and velocity information is available for the Canterbury region in contrast to the rest of New Zealand. Three specific subregions have been implemented to characterise velocities within the Canterbury region: the Canterbury Sedimentary subregion characterises Canterbury-wide sedimentary deposits; the Banks Peninsular Volcanics (BPV) subregion prescribes velocities within an outcropping volcanic formation; and the Christchurch Quaternary sedimentary subregion
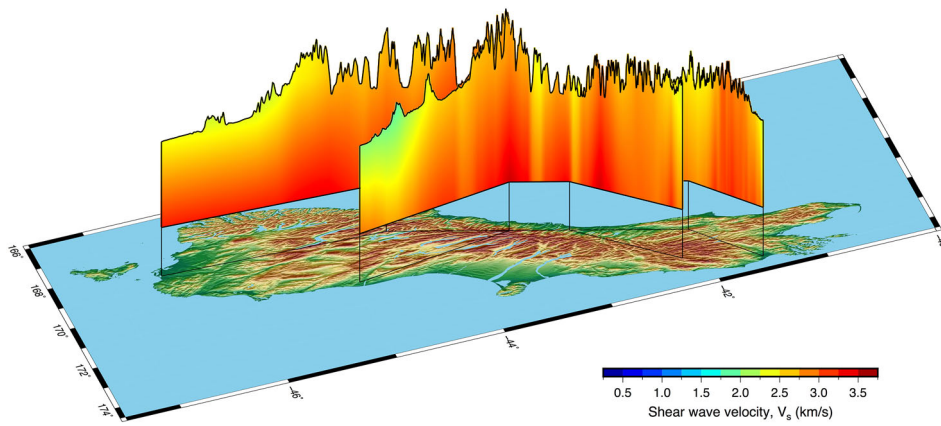
Figure 11. Velocity model fence diagram for the NZVM2.0 illustrating the velocity structure throughout the South Island to a depth of 2 km.

Table 1. Characteristics of NZVM2.0 subregion types.

Type	Features	Subregions
1	No direct measurements. Basin geometry based on topographic slope at outcrops, geologic cross sections. Generic 1D basin velocity model.	Hanmer Cheviot
2	As for 1, but incorporating direct measurements used to infer basin surface depth (e.g. ambient measurements, HVSR).	Waiau Kaikōura Marlborough
3	As for 2, but incorporating velocity profile information allowing departure from generic model.	Wellington Nelson-Tasman
4	Arbitrarily complex model, multiple geologic surfaces and specific velocity modelling.	Canterbury

details the interbedded sedimentary deposits in urban Christchurch.

These subregions utilise the geologic surfaces developed by Lee, Bradley, and McGann (2017) and Lee,

Bradley, et al. (2017) using geostatistical kriging of data aggregated from multiple sources including; seismic reflection lines, petroleum and water well logs, geotechnical CPT data, cross sections and rock outcrop data. Figure 13 illustrates the structure of Canterbury Sedimentary and Banks Peninsula Volcanic subregions as represented within NZVM2.0.

Sediments from the Neogene and Paleogene periods.
The Canterbury Sedimentary subregion characterises deposits of the Neogene-Paleogene period. The geologic surfaces that define this subregion were constructed primarily utilising seismic reflection survey lines which identify impedance contrasts associated with boundaries between geologic units with differing seismological properties (Lee, Bradley, et al. 2017). Additionally, petroleum exploration well logs and
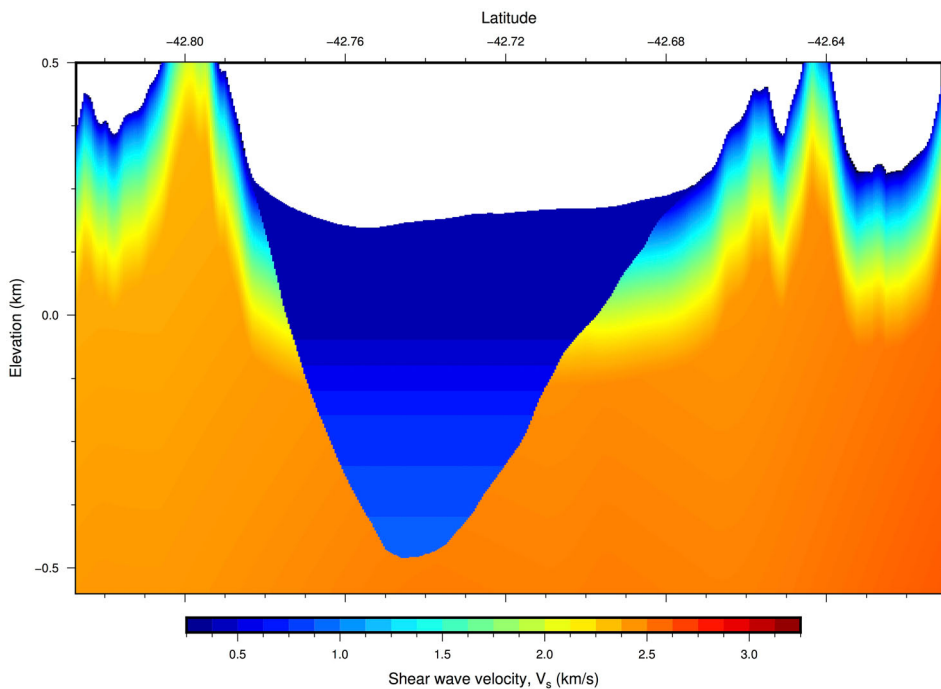

Figure 12. Velocity transect illustrating the structure of the Waiau subregion, a Type 2 characterisation. A V_{s30}-based geotechnical layer has been applied outside of the subregion.
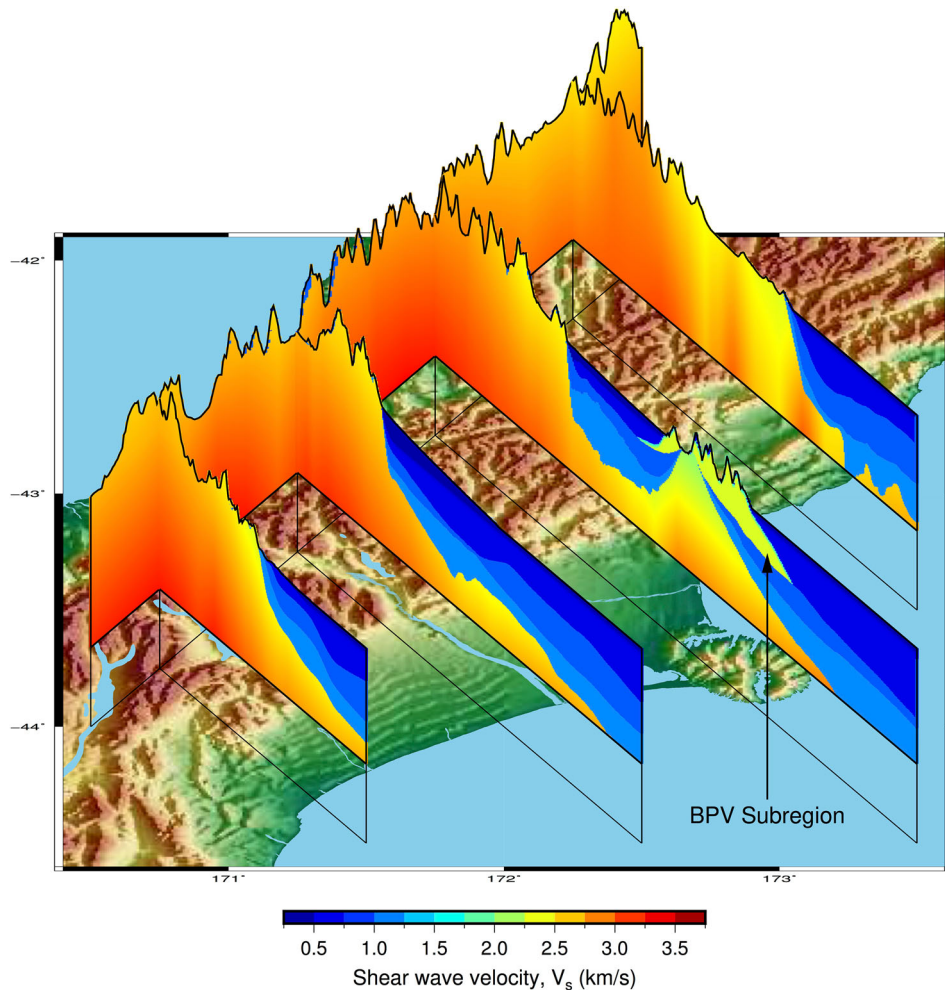
Figure 13. Velocity model fence diagram for Canterbury region illustrating the velocity structure within two subregions: the Canterbury Sedimentary subregion and the intrusive volcanic deposition forming the basis of the Banks Peninsular Volcanics subregion.

geologic outcrop data were used as additional constraints in spatially interpolating these surfaces. Three distinct layers were developed for implementation within the Canterbury Sedimentary subregion, in order of increasing depth and age these are; Pliocene Epoch, Miocene Epoch and the Paleogene Period. These layers within the context of the NZVM are referred to as the Pliocene, Miocene and the Paleogene. Four geologic surfaces are used to define these geologic layers, which collectively form the Canterbury Sedimentary subregion, constant velocities are prescribed for each layer (efforts to subsequently develop depth-dependant parameterisations are ongoing, Thomson et al. 2017). These sedimentary layers within the Canterbury Basin have significantly lower velocities than the surrounding basement and their characterisation is paramount to conducting realistic ground motion simulations in the region. Figure 13 presents velocity transects through the Canterbury subregion, the sediment layers taper to the ground surface towards the mountains in north-west of Canterbury and are of varying thickness throughout the region.

Banks Peninsula Volcanics. The development of the BPV subregion geologic surfaces utilised numerous additional datasets to those used in the construction of the Canterbury Sedimentary surfaces. Water well-logs and surface elevation contours (Brown and Weeber 1994) were used to constrain the top surface of the BPV near outcropping regions (Lee, Bradley, et al. 2017). These datasets were added to the seismic reflection and petroleum exploration well-log data to provide the necessary constraint to spatially interpolate the top surface of the BPV. As the BPV was an intrusive deposition, the bottom surface of the BPV coincides with the conclusion of the Miocene Epoch. Therefore, the bottom layer of the BPV is prescribed as the top surface of the Miocene. The BPV is prescribed in the NZVM2.0 as a single geologic layer, characterised by constant velocities with a 'weathering function' applied in the top 350 m of the subregion to reduce velocities. Figure 13 presents velocity transects through the Canterbury region, one of which transects the BPV subregion illustrating the cone-shaped structure as annotated. Explicit modelling of the BPV for ground motion simulation is important as the seismological
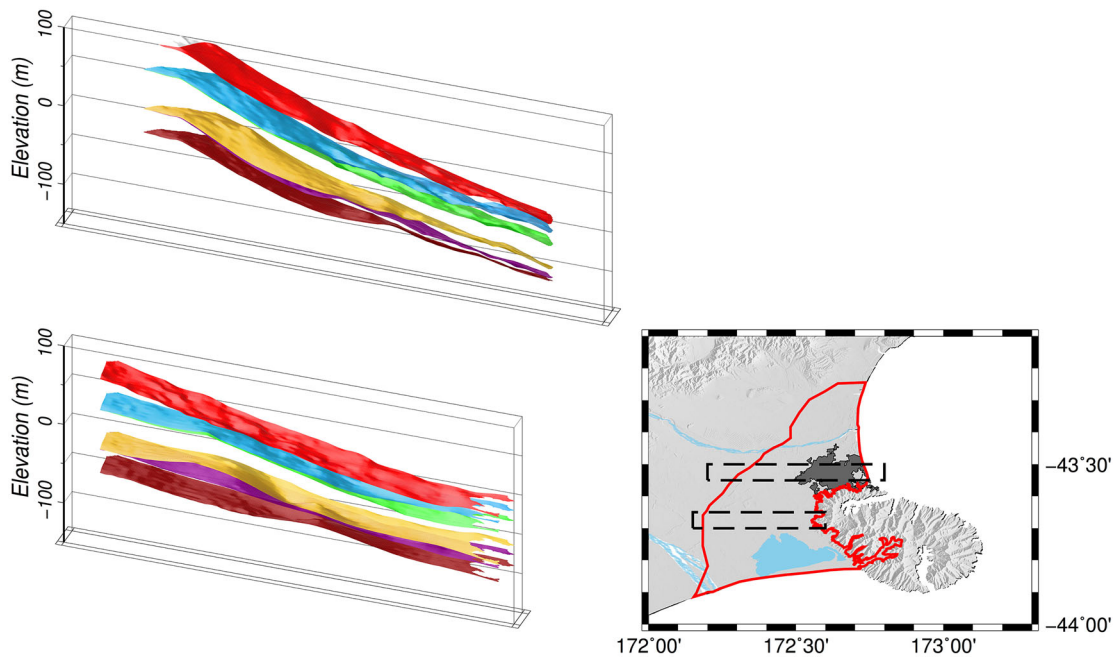
Figure 14. Velocity cross sections through the Christchurch Quaternary subregion showing the 3D interbedded layering. Fluvial gravel deposits taper to zero thickness towards the coast while marine deposits taper to zero thickness towards the Southern Alps.

properties differ significantly from that of the surrounding material and therefore have a large effect on simulated ground motions (Razafindrakoto et al. 2018).

High-resolution Quaternary sedimentary model in urban Christchurch.

A shallow subregion to characterise the interbedded Christchurch Quaternary has been implemented in NZVM2.0. The Quaternary deposits within Canterbury consist of interbedded gravels and silts sequentially deposited between glacial and interglacial periods respectively (Lee, Bradley, and McGann 2017). These interbedded layers differ significantly in composition and seismological properties resulting in alternating soft-over-stiff layering. These layers in the near surface region ($z < 200$ m) are of relatively small individual thicknesses (<30 m). Given that ground motion simulations conventionally consider a maximum frequency on the order of 1 Hz (Graves and Pitarka 2010), which for a $V_{s,min} = 500$ m/s and a grid spacing of 100 m, the effect of these layers is not explicitly captured. However, this spatial discretization, which is proportional to the maximum frequency able to be simulated, is likely to decrease in the future. Therefore, the primary application of the Christchurch Quaternary sedimentary model within the NZVM is for use in geotechnical applications such as site response analysis with the potential for this subregion to utilised within regional ground motion simulations of higher spatial resolution in the future.

A total of eight geologic layers, four gravel and four marine deposits, are modelled within the Christchurch Quaternary subregion. In order of increasing depth from the ground surface these are: Christchurch

Formation, Riccarton Gravel, Bromley Formation, Linwood Gravel, Heathcote formation, Burwood Gravel, Shirley formation and the Wainoni Gravel. Figure 14 illustrates the 3D structure of the interbedded gravel and marine formations in the Christchurch Quaternary subregion. Marine sediments, deposited when sea levels are high during interglacial periods, taper to zero thickness towards the Southern Alps. While fluvial gravels are deposited during glacial periods when ocean levels are low, tapering to zero thickness towards the present-day coastline. Velocities within these layers are characterised by simple depth-dependant functions (Thomson et al. 2017; Deschenes et al. 2018).

Geotechnical layer and offshore subregion edge smoothing

Geotechnical layer

Figure 10 illustrates that the regional tomographic model has large velocities in the near surface. Since more refined subregion models are not present everywhere, the locations outside of subregions likely have overestimated velocities in the near surface. Recognising this issue, Ely et al. (2010) developed a geotechnical layer (GTL) to adjust the velocities from regional models. This same Ely et al. (2010) model was implemented allowing additional near-surface velocity information to be integrated within the relatively low resolution tomographic model (i.e. outside of explicitly modelled subregions). The GTL applies a quadratic taper to reduce velocities in the top 350 m of the tomographic model to match the V_{s30} value at a site. The GTL utilises a V_{s30} model (Foster 2017), which

combines topographic slope, surficial geology and direct observations to generate a full coverage New Zealand specific V_{s30} model. Figure 12 illustrates the GTL reducing nearsurface velocities in the tomographic model outside of the Waiau subregion.

Offshore subregion edge smoothing
Subregions model continuous geologic deposits which, in the onshore case; typically taper to zero thickness (i.e. at rock outcrops) while for the offshore case, subregions can have non-zero thickness where they terminate an example is shown in Figure 15. This offshore subregion 'edge' is non-physical and represents a large velocity contrast which has an undesirable effect on simulations. The method implemented for reducing the velocity contrast at the subregion-tomography transition is to linearly smooth this velocity transition over a 10 km distance. This smoothing regime was implemented to reduce the effect of undesirable offshore reverberations and is designed to occur at a sufficient distance as to not affect onshore motions.

Outputs from the model

The NZVM was developed for multiple use cases including ground motion simulation, site response analysis and generation of seismic velocity contour maps. Applying the NZVM for use in these applications yield different output formats, these formats vary by application and are briefly discussed in subsequent subsections.

3D gridded velocity model
The NZVM has been implemented to construct a velocity model on a 3D grid to be used in ground motion simulations. The resulting velocity model is saved as three binary files, one for each the P-wave and S-wave velocities, and the density. In addition to saving the model for use in ground motion simulation, the NZVM is able to read a saved velocity model and interpolate velocity transects to visualise the model which enables the velocity structure to be investigated

for different model versions, grid-spacings and topographic representations (see Figure 8).

Prescription of velocities to a list of gridpoints
The NZVM can be used to prescribe velocities to a file containing a list of one or more gridpoints. This is useful for cases in which the exact velocity at a gridpoint is required or for prescription of velocities to a non-uniform grid (e.g. Tu et al. 2006; Taborda et al. 2010). The non-uniform grid can be generated by external meshing software, saved to file and used as an input to the NZVM, which then assigns velocities to these gridpoints.

Seismic velocity profiles at specific latitude-longitude locations
To perform a one-dimensional site response analysis at a given site, the local velocity structure must be known. Therefore, one output from the NZVM made available is 1D site-specific velocity profiles which can be used in seismic site response modelling. The 1D profiles from the NZVM also include the depths of geologic surfaces used in the construction of subregions in addition to the velocity structure. These geologic surface depths (such as the depth of the basement, and depth to interbedded sedimentary layers) are also instrumental as constraints for processing regional geophysical data (e.g. Teagu et al. 2017; Deschenes et al. 2018).

Generation of velocity transects
Velocity transects through saved velocity models provide useful information as to the velocity structure represented within the saved model, however the resolution of these transects is equivalent to the grid-spacing of the saved model and these transects have a relatively low resolution (>100 m) which, is insufficient for visualisation purposes where a high resolution velocity structure (<10 m) representation is desirable. Therefore the NZVM is able to generate velocity transects directly based on two pairs of latitude and longitude coordinates and a user specified resolution,
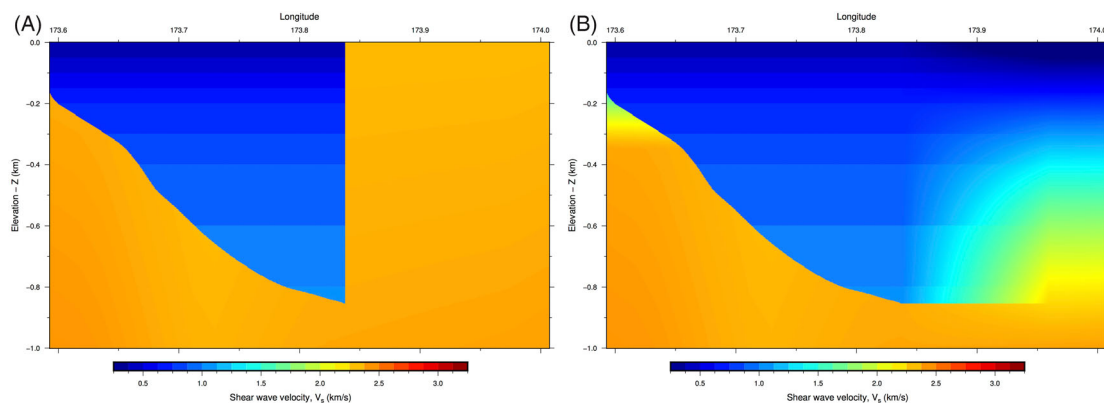

Figure 15. Offshore subregion-edge smoothing: **A,** without offshore and **B,** with a linear smoothing regime and GTL.
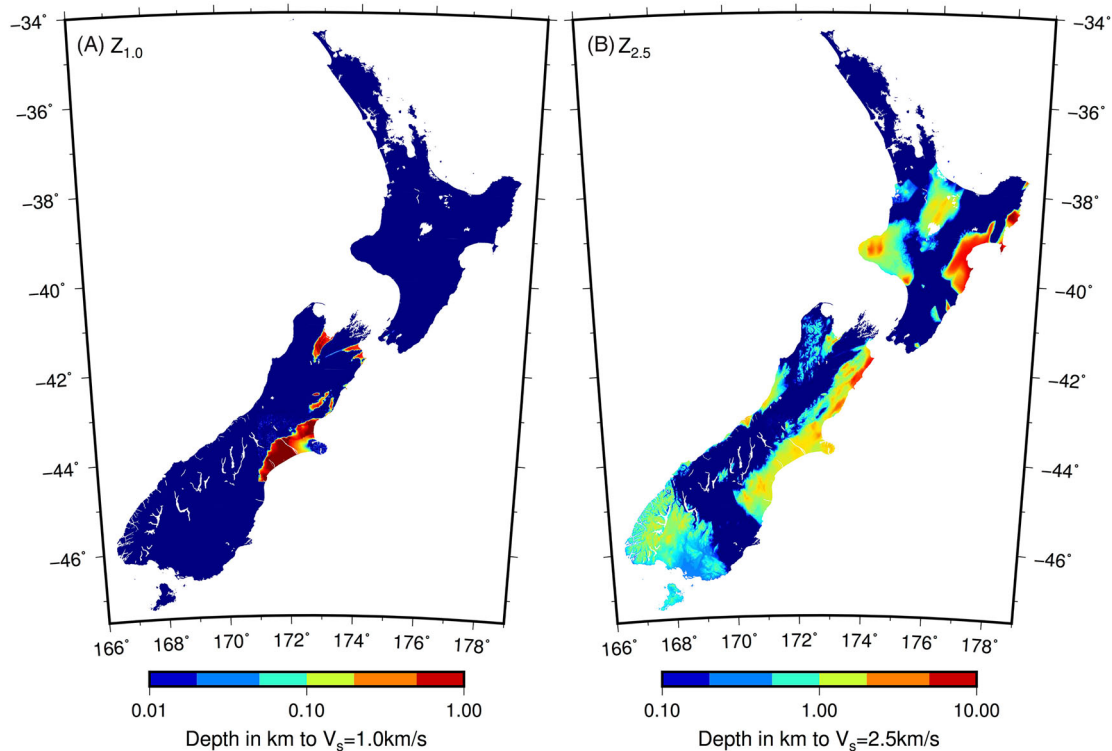
Figure 16. Seismic velocity contour maps generated by the NZVM2.0: **A,** the depth to shear wave velocity 1.0 km/s ($Z_{1.0}$) and **B,** the depth to 2.5 km/s ($Z_{2.5}$).

enabling the meter-scale velocity structure to be visualised.

Seismic velocity contour maps

Seismic velocity contour maps illustrating regional shear wave velocity characteristics can be utilised in empirical ground motion models to incorporate the effect of sedimentary basins (e.g. Campbell and Bozorgnia 2008; Day et al. 2008; Abrahamson et al. 2014; Chiou and Youngs 2014). The NZVM allows for the generation of two different types of contour maps based on either the shear wave velocity within the near surface region (V_{s30} and V_{s500}, the time-averaged shear wave velocity over the top 30 or 500 m respectively) or the depth to a shear wave velocity threshold ($Z_{1.0}$ and $Z_{2.5}$, the depth to shear wave velocity of 1 km/s or 2.5 km/s respectively).

Figure 16 illustrates seismic velocity contour maps of $Z_{1.0}$ and $Z_{2.5}$ generated from the NZVM2.0. The $Z_{1.0}$ map (approximately geotechnical depth to bedrock (Abrahamson et al. 2014)) shows that only within modelled subregions are S-wave surface velocities below 1 km/s, additionally the effect of the intrusive Banks Peninsula Volcanics deposit can be seen as this subregion has relatively high velocities compared with the surrounding Canterbury deposits. Within the $Z_{2.5}$ map the depth to 2.5 km/s S-wave velocity varies from 0–11 km and loosely aligns with our knowledge of geologic terranes (Mortimer 2004) indicating the regional crustal model of Eberhart-Phillips et al. (2010) is representative of the regional geology.

Use in ground motion simulation

Ground motion simulations of prospective (e.g. Bradley, Bae, et al. 2017) or historic earthquakes (e.g. Bradley, Razafindrakoto, et al. 2017; Razafindrakoto et al. 2018) have been conducted utilising the NZVM and the Graves and Pitarka (2010) methodology. Simulated motions are able to be utilised in numerous engineering applications ranging from hazard assessment to disaster preparedness in addition to providing valuable insights into fault rupture and seismic wave propagation processes. Simulation of historic earthquakes can provide insights into the earthquakes that have previously occurred and can be used to validate both the velocity model and simulation methodology through comparison of simulated and observed ground motions. Prospective scenario-based ground motion simulations can be utilised to assess the impact of different rupture scenarios (e.g. hypocentre locations and fault parameters) and their subsequent effects.

Recent advances in the computational processing power and the availability of HPC resources allow for multiple large scale physics-based ground motion simulations to be conducted. Physics-based probabilistic seismic hazard maps can be generated for a region by combining the results of ground motion simulations for all faults affecting the region (e.g. Graves et al. 2011; Tarbali et al. 2018). Given the advancements in validating physics-based methodologies, it is expected that ground motion simulations will play an ever-increasing role in the assessment of seismic hazards. Simulated

motions additionally can be compared with empirical ground motion models and hence illustrate possible biases of deficiencies in these equations and the current code provisions that utilise them.

Conclusions

This paper has presented a generalised and extensible methodology and computational framework for crustal velocity modelling, and the development of a New Zealand Velocity Model (NZVM). The methodology utilises modular subregions which are embedded within a tomographic model covering NZ in its entirety, with the flexibility and extensibility to add and change subregions and velocity parametrisations in future model versions. The NZVM has a variety of use cases including ground motion simulation, site response analysis, earthquake relocation and for seismic hazard analysis.

The modularity of the NZVM allows for surfaces, subregions and velocity pa-rameterisations to be modified or added in the future. Figure 9 illustrates the locations of subregions of interest immediately planned for future NZVM versions. These regions are currently characterised by the regional travel time tomographical model of Eberhart-Phillips et al. (2010) hence, the addition of subregion models to the NZVM will improve the quality of simulated ground motions within these regions. The open-source NZVM code-base (see Data and resources) enables additional subregions to be implemented by the wider research community.

The regional travel time tomography model used to prescribe basement velocities throughout the NZVM (Eberhart-Phillips et al. 2010) can be significantly improved through full waveform three dimensional tomographic inversion (F3DT) (e.g Lee et al. 2014) which can be used to identify and constrain lower velocity regions. Through the application of F3DT, the velocity structure of the NZVM can be subsequently improved beyond what is capable using travel-time tomographic inversion (e.g. Lee and Chen 2016).

Data and resources

NZVM2.0 is available in the programming language C with associated files on github at https://github.com/ucgmsim/Velocity-Model.

Figures were prepared using Generic Mapping Tools (https://gmt.soest.hawaii.edu/), MATLAB (https://mathworks.com/products/matlab.html) and draw.io (https://www.draw.io/).

Acknowledgements

Disclosure statement

No potential conflict of interest was reported by the authors.

References

Aagaard BT, Brocher TM, Dolenc D, Dreger D, Graves RW, Harmsen S, Hartzell S, Larsen S, Zoback ML. 2008. Ground-motion modeling of the 1906 San Francisco earthquake, part I: validation using the 1989 Loma Prieta earthquake. Bulletin of the Seismological Society of America. 98(2):989–1011.

Aagaard BT, Hall JF, Heaton TH. 2001. Characterization of near-source ground motions with earthquake simulations. Earthquake Spectra. 17(2):177–207.

Abrahamson NA, Silva WJ, Kamai R. 2014. Summary of the ASK14 ground motion relation for active crustal regions. Earthquake Spectra. 30(3):1025–1055.

Barker DH, Sutherland R, Henrys S, Bannister S. 2009. Geometry of the Hikurangi subduction thrust and upper plate, North Island, New Zealand. Geochemistry, Geophysics, Geosystems. 10(2):n/a–n/a.

Begg J, Johnston M. 2000. Geology of the Wellington area. Institute of Geological and Nuclear Sciences 1: 250 000 geological map 10. Lower Hutt: Institute of Geological and Nuclear Sciences Ltd; p. 64.

Bradley BA, Bae SE, Polak V, Lee RL, Thomson EM, Tarbali K. 2017. Ground motion simulations of great earthquakes on the Alpine fault: effect of hypocentre location and comparison with empirical modelling. New Zealand Journal of Geology and Geophysics. 60(3):188–198.

Bradley BA, Razafindrakoto HN, Polak V. 2017. Ground-motion observations from the 14 November 2016 M_w 7.8 Kaikoura, New Zealand, earthquake and insights from broadband simulations. Seismological Research Letters. 88(3):740–756.

Brocher TA. 2005. Empirical relations between elastic wave-speeds and density in the earth's crust. Bulletin of the Seismological Society of America. 95(6):2081–2092.

Brown L, Weeber J. 1994. Hydrogeological implications of geology at the boundary of Banks Peninsula volcanic rock aquifers and Canterbury Plains fluvial gravel aquifers. New Zealand Journal of Geology and Geophysics. 37(2):181–193.

Campbell KW, Bozorgnia Y. 2008. NGA ground motion model for the geometric mean horizontal component of PGA, PGV, PGD and 5ranging from 0.01 to 10 s. Earthquake Spectra. 24(1):139–171.

Chaljub E, Maufroy E, Moczo P, Kristek J, Hollender F, Bard PY, Priolo E, Klin P, de Martin F, Zhang ZG, et al. (2015). 3- d numerical simulations of earthquake ground motion

in sedimentary basins: testing accuracy through stringent models. Geophysical Journal International. 201(1):90–111.

Chiou BS-J, Youngs RR. 2014. Update of the Chiou and Youngs NGA model for the average horizontal component of peak ground motion and response spectra. Earthquake Spectra. 30(3):1117–1153.

Cui Y, Olsen KB, Jordan TH, Lee K, Zhou J, Small P, Roten D, Ely G, Panda DK, Chourasia A. 2010. Scalable earthquake simulation on petascale supercomputers. IEEE; p. 1–20.

Davy B, Hoernle K, Werner R. 2008. Hikurangi Plateau: crustal structure, rifted formation, and Gondwana subduction history. Geochemistry, Geophysics, Geosystems. 9(7):n/a–n/a.

Day SM, Graves R, Bielak J, Dreger D, Larsen S, Olsen KB, Pitarka A, Ramirez-Guzman L. 2008. Model for basin effects on long-period response spectra in southern California. Earthquake Spectra. 24(1):257–277.

Deschenes MR, Wood CM, Wotherspoon LM, Bradley BA, Thomson EM. 2018. Development of deep shear wave velocity profiles in the Canterbury Plains, New Zealand. Earthquake Spectra. 34(3):1065–1089.

Eberhart-Phillips D, Reyners M, Bannister S, Chadwick M, Ellis S. 2010. Establishing a versatile 3-D seismic velocity model for New Zealand. Seismological Research Letters. 81(6):992–1000.

Ely GP, Jordan T, Small P, Maechling PJ. 2010. A VS 30-derived near-surface seismic velocity model. Abstract S51A-1907, Fall Meeting; AGU San Francisco, CA.

Foster K. 2017. A Vs30 map for New Zealand. Poster session presented at: QuakeCoRE Annual Meeting; Sep 4–6; Wairakei Resort; Taupo, New Zealand.

Frankel A, Stephenson W. 2000. Three-dimensional simulations of ground motions in the Seattle region for earthquakes in the Seattle fault zone. Bulletin of the Seismological Society of America. 90(5):1251–1267.

Goto H, Sawada S, Morikawa H, Kiku H, Ozalaybey S. 2005. Modeling of 3D subsurface structure and numerical simulation of strong ground motion in the Adapazari Basin during the 1999 Kocaeli earthquake, Turkey. Bulletin of the Seismological Society of America. 95(6):2197–2215.

Graves RW. 1996. Simulating seismic wave propagation in 3D elastic media using staggered-grid finite differences. Bulletin of the Seismological Society of America. 86(4):1091–1106.

Graves R, Jordan TH, Callaghan S, Deelman E, Field E, Juve G, Kesselman C, Maechling P, Mehta G, Milner K, et al. 2011. Cybershake: a physics-based seismic hazard model for Southern California. Pure and Applied Geophysics. 168(3):367–381.

Graves RW, Pitarka A. 2010. Broadband ground-motion simulation using a hybrid approach. Bulletin of the Seismological Society of America. 100(5a):2095–2123.

Harmsen S, Hartzell S, Liu PC. 2008. Simulated ground motion in Santa Clara valley, California, and vicinity from M> = 6.7 scenario earthquakes. Bulletin of the Seismological Society of America. 98(3):1243–1271.

Hauksson E, Haase JS. 1997. Three-dimensional V_p and V_p/V_s velocity models of the Los Angeles basin and central Transverse Ranges, California. Journal of Geophysical Research: Solid Earth. 102(B3):5423–5453.

Horspool N, Savage M, Bannister S. 2006. Implications for intraplate volcanism and back-arc deformation in northwestern New Zealand, from joint inversion of receiver functions and surface waves. Geophysical Journal International. 166(3):1466–1483.

Kagawa T, Zhao BM, Miyakoshi K, Irikura K. 2004. Modeling of 3D basin structures for seismic wave simulations based on available information on the target area: case study of the Osaka basin, Japan. Bulletin of the Seismological Society of America. 94(4):1353–1368.

Kohler MD, Magistrale H, Clayton RW. 2003. Mantle heterogeneities and the SCEC reference three-dimensional seismic velocity model version 3. Bulletin of the Seismological Society of America. 93(2):757–774.

Komatitsch D, Tromp J. 1999. Introduction to the spectral element method for three-dimensional seismic wave propagation. Geophysical Journal International. 139(3):806–822.

Lee E-J, Chen P. 2016. Improved basin structures in Southern California obtained through full-3D seismic waveform tomography (F3DT). Seismological Research Letters. 87(4):874–881.

Lee EJ, Chen P, Jordan TH, Maechling PB, Denolle MAM, Beroza GC. 2014. Full-3-D tomography for crustal structure in Southern California based on the scattering-integral and the adjoint-wavefield methods. Journal of Geophysical Research: Solid Earth. 119(8):6421–6451.

Lee RL, Bradley BA, Ghisetti FC, Thomson EM. 2017. Development of a 3D velocity model of the Canterbury, New Zealand, region for broadband ground-motion simulation. Bulletin of the Seismological Society of America. 107(5):2131–2150.

Lee RL, Bradley BA, McGann CR. 2017. 3D models of Quaternary-aged sedimentary successions within the Canterbury, New Zealand region. New Zealand Journal of Geology and Geophysics. 60(4):320–340.

Lee RL, Bradley BA, Stafford PJ, Graves RW, Rodriguez-Marek A. 2018. Hybrid broadband ground motion simulation validation in the Canterbury, New Zealand Region. Bulletin of the Seismological Society of America, TBD: TBD. Submitted.

Magistrale H, Day S, Clayton RW, Graves R. 2000. The SCEC southern California reference three-dimensional seismic velocity model version 2. Bulletin of the Seismological Society of America. 90(6):S65–S76.

Magistrale H, McLaughlin K, Day S. 1996. A geology-based 3D velocity model of the Los Angeles basin sediments. Bulletin of the Seismological Society of America. 86(4):1161–1166.

Maufroy E, Chaljub E, Hollender F, Kristek J, Moczo P, Klin P, Priolo E, Iwaki A, Iwata T, Etienne V, et al. 2015. Earthquake ground motion in the Mygdonian basin, Greece: The E2VP verification and validation of 3D numerical simulation up to 4 Hz. Bulletin of the Seismological Society of America. 105(3):1398–1418.

McMahon R, Wotherspoon L. 2017. Nelson Tasman site classification study. Poster session presented at: QuakeCoRE Annual Meeting; Sep 4–6; Wairakei Resort; Taupo, New Zealand.

Molinari I, Argnani A, Morelli A, Basini P. 2015. Development and testing of a 3D seismic velocity model of the po plain sedimentary Basin, Italy. Bulletin of the Seismological Society of America. 105(2a):753–764.

Molinari I, Morelli A. 2011. EPcrust: a reference crustal model for the European Plate. Geophysical Journal International. 185(1):352–364.

Mortimer N. 2004. New Zealand's geological foundations. Gondwana Research. 7(1):261–272.

Olsen KB, Day SM, Minster JB, Cui Y, Chourasia A, Faerman M, Moore R, Maechling P, Jordan T. 2006. Strong shaking in Los Angeles expected from southern San Andreas earthquake. Geophysical Research Letters. 33(7):L07305.

Parsons T, Blakely RJ, Brocher TM. 2001. A simple algorithm for sequentially incorporating gravity observations in seismic traveltime tomography. International Geology Review. 43(12):1073–1086.

Pitarka A, Graves R, Somerville P. 2004. Validation of a 3D velocity model of the Puget Sound region based on modeling ground motion from the 28 February 2001 Nisqually earthquake. Bulletin of the Seismological Society of America. 94(5):1670–1689.

Ramírez-Guzmán L, Boyd OS, Hartzell S, Williams RA. 2012. Seismic velocity model of the central United States (version 1): Description and simulation of the 18 April 2008 Mt. Carmel, Illinois, earthquake. Bulletin of the Seismological Society of America. 102(6):2622–2645.

Rattenbury M, Cooper R, Johnston M. 1998. Geology of the Nelson area. Institute of Geological and Nuclear Sciences 1: 250 000 geological map 9. Lower Hutt: Institute of Geological and Nuclear Sciences Ltd.

Rattenbury M, Townsend D, Johnston M. 2006. Geology of the Kaikoura area. Institute of Geological and Nuclear Sciences 1: 250 000 geological map 13. Lower Hutt: Institute of Geological and Nuclear Sciences Ltd.

Razafindrakoto HNT, Bradley BA, Graves RW. 2018. Broadband groundmotion simulation of the 2011 Mw 6.2 Christchurch, New Zealand, earthquake- broadband groundmotion simulation of the 2011 Mw 6.2 Christchurch earthquake. Bulletin of the Seismological Society of America. 108(4):2130–2147.

Rodgers A, Petersson NA, Nilsson S, Sjogreen B, McCandless K. 2008. Broadband waveform modeling of moderate earthquakes in the San Francisco Bay Area and preliminary assessment of the USGS 3D seismic velocity model. Bulletin of the Seismological Society of America. 98(2):969–988.

Roten D, Fah D, Olsen KB, Giardini D. 2008. A comparison of observed and simulated site response in the Rhone valley. Geophysical Journal International. 173(3):958–978.

Roten D, Olsen KB, Day SM, Cui Y, Fah D. 2014. Expected seismic shaking in Los Angeles reduced by San Andreas fault zone plasticity. Geophysical Research Letters. 41(8):2769–2777.

Semmens S, Dellow G, Perrin N. 2010. Its our fault - geological and geotechnical characterisation of the Wellington central business district. GNS Science Consultancy Report 2010/176.

Shaw JH, Plesch A, Tape C, Suess MP, Jordan TH, Ely G, Hauksson E, Tromp J, Tanimoto T, Graves R, et al. 2015. Unified structural representation of the Southern California crust and upper mantle. Earth and Planetary Science Letters. 415:1–15.

Süss MP, Shaw JH. 2003. P wave seismic velocity structure derived from sonic logs and industry reflection data in the Los Angeles basin, California. Journal of Geophysical Research: Solid Earth. 108(B3):1–18.

Taborda R. 2014. Evaluation of attenuation models (Q-Vs relationships) used in physics-based ground-motion earthquake simulation through validation with data. Report, University of Memphis; Memphis; TN 38152, USA.

Taborda R, Bielak J. 2014. Ground-motion simulation and validation of the 2008 Chino Hills, California, earthquake using different velocity models. Bulletin of the Seismological Society of America. 104(4):1876–1898.

Taborda R, López J, Karaoglu H, Urbanic J, Bielak J. 2010. Speeding up finite element wave propagation for large-scale earthquake simulations. Parallel Data Laboratory Tech. Rept. CMUPDL-10-109.

Tarbali K, Bradley B, Huang J, Polak V, Lagrava D, Motha J, Bae S. 2018. Cybershake NZ v17.9: New Zealand simulation-based probabilistic seismic hazard analysis. Proceedings of 16th European Conference on Earthquake Engineering - Thessaloniki, Greece.

Teague D, Cox B, Bradley B, Wotherspoon L. 2017. Development of deep shear wave velocity profiles with estimates of uncertainty in the complex interbedded geology of Christchurch, New Zealand. Earthquake Spectra. 34(2):639–672.

Thomson E, Bradley B, Wotherspoon L, Cox B, Wood C. 2017. Generalised parametic function and spatial correlations for seismic velocities in the Canterbury region based on dynamic site characterisation. Poster session presented at: QuakeCoRE Annual Meeting; Sep 4–6; Wairakei Resort; Taupo, New Zealand.

Tu T, Yu H, Ramirez-Guzman L, Bielak J, Ghattas O, Ma K-L, O'hallaron DR. 2006. From mesh generation to scientific visualization: an end-to-end approach to parallel supercomputing. Proceedings of the 2006 ACM/IEEE conference on Supercomputingl ACM; p. 91.

Wood R, Woodward D. 2002. Sediment thickness and crustal structure of offshore western New Zealand from 3D gravity modelling. New Zealand Journal of Geology and Geophysics. 45(2):243–255.